

5.1 ESTIMATIONS OF FOREST FIRE SMOKE FORCING FROM SURFACE MEASUREMENTS, SATELLITE DATA, AND TRAJECTORY MODELING

Stephen J. Cox

Analytical Services and Materials, Inc., Hampton, VA

P.W. Stackhouse, Jr., Bryan A. Baum, R. Bradley Pierce, V.L. Harvey
Atmospheric Sciences Division, NASA Langley Research Center, Hampton, VA

Marc Chiacchio, J. Colleen Mikovitz
Analytical Services and Materials, Inc., Hampton, VA

1. INTRODUCTION

The 1989 fire season in Manitoba, Canada set a record for both the number of fires and for burned area. Evacuation of several communities was required during the July 21-23 period of heaviest burning. Smoke was widespread over a large area during July and August.

Forest fire smoke can have an important impact on the atmospheric radiative transfer over the affected areas. Both the surface and top-of-atmosphere radiation fluxes can be greatly affected for periods of months. Here we present results of a study to assess the direct radiative forcing from the 1989 Manitoba fires. We use AVHRR Local Area Coverage (LAC) data and a grouped threshold approach (Baum and Trepte 1999) to detect fire, smoke, burn scar, cloudy, and clear pixels. The fire pixels are used to initialize a transport model. Forcings are calculated at several Canadian surface radiometer sites, and results are compared to the trajectory model output and the TOMS aerosol index.

2. SCENE IDENTIFICATION

Baum and Trepte (1999) developed a scene identification algorithm using AVHRR radiances in the 5 standard channels (0.63 μm , 0.86 μm , 3.7 μm , 11 μm , and 12 μm). Pixels are identified as smoke, fire, burn scar, cloudy, or clear. The algorithm is currently limited to forest surfaces, which are relatively uniform, dark, and cool. The primary challenge is the differentiation between smoke and cloud. Reflectances and brightness temperatures are compared to expected clear sky values, and threshold tests are applied to separate cloudy pixels from smoke pixels. The threshold tests are derived from previous studies (e.g. Kaufman *et al.* 1990) and further operational testing and calculation.

3. SMOKE OPTICAL DEPTH RETRIEVAL

For those pixels identified as smoke, optical depths are estimated in order to perform a radiative forcing calculation. Optical depths are calculated using channel 1 reflectances and viewing geometry (solar zenith angle, viewing zenith angle, relative azimuth angle). A lookup table of optical properties was generated using the Discrete Ordinate (DISORT) radiative transfer model (Stamnes *et al.* 1988), using correlated- k gaseous absorption and Rayleigh scattering. The optical properties of smoke were computed as a lognormal mixture of soot, soluble and insoluble particles such that the single scatter albedo was 0.9.

On the basis of retrieved aerosol optical thickness, the AVHRR pixels are binned subsequently into thin ($\tau < 0.1$), medium ($0.1 < \tau < 0.5$), medium heavy ($0.5 < \tau < 1.0$), and heavy ($\tau > 1.0$) smoke. By separating the pixels according to the magnitude of the optical thickness, we mitigate uncertainties caused by variations in surface albedo and in the composition of the smoke aerosol used to generate the scattering properties. In addition, there is an asymptotic loss of sensitivity of radiance with increasing optical depth.

4. SHORTWAVE FORCING

Shortwave forcing calculations were performed using a version of the Fu-Liou radiative transfer code LAC smoke pixels were regridded over the Manitoba scene onto a $0.25^\circ \times 0.25^\circ$ grid. For each bin, a representative optical depth was chosen (.08, .45, .85, 1.1 for thin, medium, medium heavy, and heavy, respectively). The smoke was modeled in the Fu-Liou code as a mixture of 90% continental aerosol and 10% soot, which gives a 0.9 single scatter albedo used in the optical depth retrieval. A forcing for each optical depth bin was calculated for all quarter degree cells for each day that AVHRR data was available from July 1 through August 13, 1989. The forcing was weighted by the fractional smoke coverage of each optical depth bin. No attempt was made to model smoke forcing for cloudy pixels.

Corresponding author address: Stephen J. Cox,
Analytical Services & Materials, Inc., 1 Enterprise
Pkwy., Suite 300, Hampton, VA 23666
e-mail: s.j.cox@larc.nasa.gov

Over the heavy smoke area near the fires, the smoke forcing is as high as 195 Wm^{-2} , and averages 68 Wm^{-2} for the smoke covered areas. For the available days from July 1 to August 13, a total of $\sim 968,000 \text{ km}^2$ in the area from $48\text{--}60^\circ\text{N}$, $79\text{--}103^\circ\text{W}$ had smoke coverage for at least one day. For the entire period, the smoke-affected area had an average surface forcing of 8.2 Wm^{-2} and an average TOA forcing of 2.5 Wm^{-2} . This indicates substantial atmospheric absorption by the smoke.

5. TRAJECTORY MODELING

The LaRC Trajectory Model (LTM, Pierce et al., 1997) was seeded with fire pixels from the scene identification algorithm. The model was run in time-forward mode with meteorological data from the European Centre for Medium-Range Weather Forecasts 15-year reanalysis (ERA-15). Air parcels were traced from fire regions over a period of five days globally on a 2.5 degree equal area grid. Areas with large numbers of trajectories originating on boundary layer air in fire regions were considered likely to be influenced by smoke. Trajectories passing within 2 degrees of Canadian surface radiometer sites were counted for each 12 hour period in the July-August 1989 fire period.

6. COMPARISONS TO SURFACE MEASUREMENTS

Hourly downward shortwave flux measurements from 24 stations throughout Canada were analyzed for possible detection of effects from forest fire smoke. First a theoretical clean-sky surface flux (i.e., with no aerosols or clouds) for each site and day was calculated with the Fu-Liou radiation code using TOMS ozone values and GEOS-1 meteorology.

The station data were then screened for clouds. In the absence of reliable cloud cover data, a proxy was developed for detecting cloud-free days. A fifth-order polynomial was fit to the daylight station data, and days where the goodness of fit was better than a threshold value were considered cloud-free.

Figures 1 and 2 show the results of this approach for Fredericton, New Brunswick, and Moosonee, Ontario for the July 22-25, 1989 period, a relatively clear but smoky time frame. Moosonee is under thick smoke for this period, as indicated by the large number of trajectories initiated on fire pixels, and confirmed by the TOMS Aerosol Index product. There is a large difference between the station measured flux and the clean sky flux. July 23 shows a local noon forcing of 250 Wm^{-2} . Days outside the fire period show a clean sky-station difference of approximately 40 Wm^{-2} , indicating that the smoke is responsible for 210 Wm^{-2} above the background aerosol. The forcing calculations described in Section 4 show a July 23, 18Z (near local noon)

smoke forcing of 150 Wm^{-2} . Uncertainties in the retrieved optical depth, smoke optical properties, background aerosol, and surface measurements can account for the disparity.

Fredericton is far outside the main influence of the smoke. However, during the July 22-25 period, trajectory modeling indicates that a thin plume of smoke extended thousands of kilometers downstream, and affected Fredericton. The station data confirms. July 22 shows a noon forcing of 154 Wm^{-2} . Later in the period when the plume moved away, the surface forcing returned to a background level of approximately 150 Wm^{-2} .

Results from several sites are shown in Tables 1 and 2. Outlook, SK lies well to the west of the fire area and is not affected by smoke. Winnipeg is under moderate smoke in late July, and TOMS AI, the trajectory model and the surface data all see the effect. Big Trout Lake, ON sees the most smoke trajectories from the model, a strong TOMS signal, and a 228 Wm^{-2} local noon forcing. The tools are in general agreement in identifying the smoke-affected areas.

7. CONCLUSION

The results presented here have shown that smoke aerosol events from forest fires may have significant areal and temporal effects on the radiation budget. Use of a combination of tools, including trajectory modeling, satellite retrievals, radiative transfer modeling, and station radiometer data can allow identification of these events, and estimations of their radiative effects.

8. ACKNOWLEDGMENTS

Funding for this research was obtained through NASA grant Aero98-0104-0103 (NRA-97-MTPE-16) in association with the GEWEX Global Aerosol Climatology Project.

9. REFERENCES

- Baum, B.A. and Q. Trepte, 1999: A grouped threshold approach for scene identification in AVHRR imagery. *J. Atmos. and Ocean. Tech.*, **16**, 793-800.
- Fu, Q. and K.N. Liou, 1993: Parameterization of the radiative properties of cirrus clouds. *J. Atmos. Sci.*, **50**, 2008-2025.
- Fu, Q., and K.-N. Liou, 1992: On the correlated k-distribution method for radiative transfer in nonhomogenous atmospheres. *J. Atmos. Sci.*, **49**, 2139-2156.
- Kaufman, Y.J., C.J. Tucker, and I. Fung, 1990: Remote sensing of biomass burning in the tropics. *J. Geophys. Res.*, **95**, 9927-9939.

Pierce, R.B., J.-U. Grooss, W.L. Grose, J.M. Russell III, P.J. Crutzen, T.D. Fairlie, G. Lingenfelter, 1997: Photochemical calculations along air mass trajectories during ASHOC/MAESA, *J. Geophys. Res.*, **102**, 13,153-13,167.

Stamnes, K., S.-C. Tsay, W. Wiscombe, and K. Jayaweera, 1988: Numerically stable algorithm for discrete-ordinate-method radiative transfer in multiple scattering and emitting layered media. *Appl. Opt.*, **27**, 2502-2509.

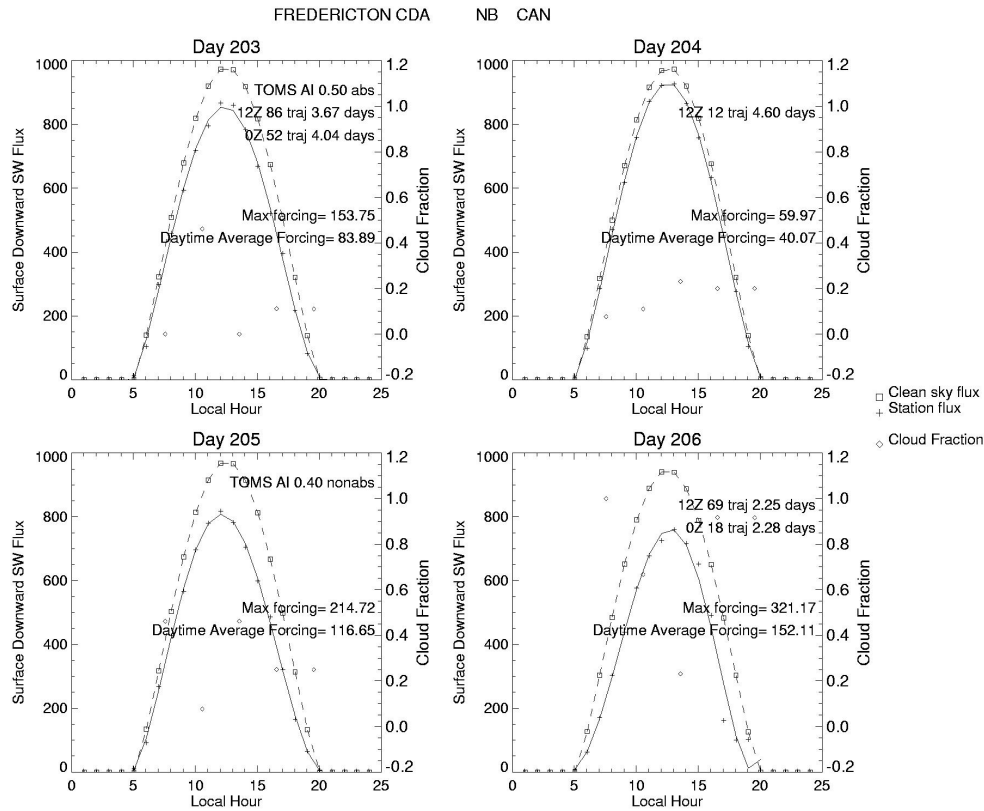


Fig. 1. Hourly time series of downward surface shortwave flux, and 3-hrly ISCCP cloud fraction for Fredericton, New Brunswick, July 22-25, 1989. The fit to the station data is a 5th-order polynomial and the goodness of fit is used to identify cloud-free days. The difference between the theoretical clean-sky flux and the surface flux is considered to be due to smoke and background aerosol. Number of trajectories initialized on fire pixels and the age of those trajectories is also given, as is the TOMS Aerosol Index for that day.

Site	Case	Max forcing (W m ⁻²) Clean - obs.	Integrated daylight forcing (W m ⁻²)
Outlook, SK	7/22 Clear-no smoke	52	27
Moosonee, ON	7/21 Thick smoke	155	101
	7/22 Thick smoke	293	157
	7/23 Thick smoke	250	145
Fredericton, NB	7/21 Thin smoke	77	37
	7/22 Thick smoke	154	83
	7/23 Thick smoke	215	117

Table 1. Estimated smoke forcing from station data and theoretical clean-sky calculations for selected stations and days during intense smoke period.

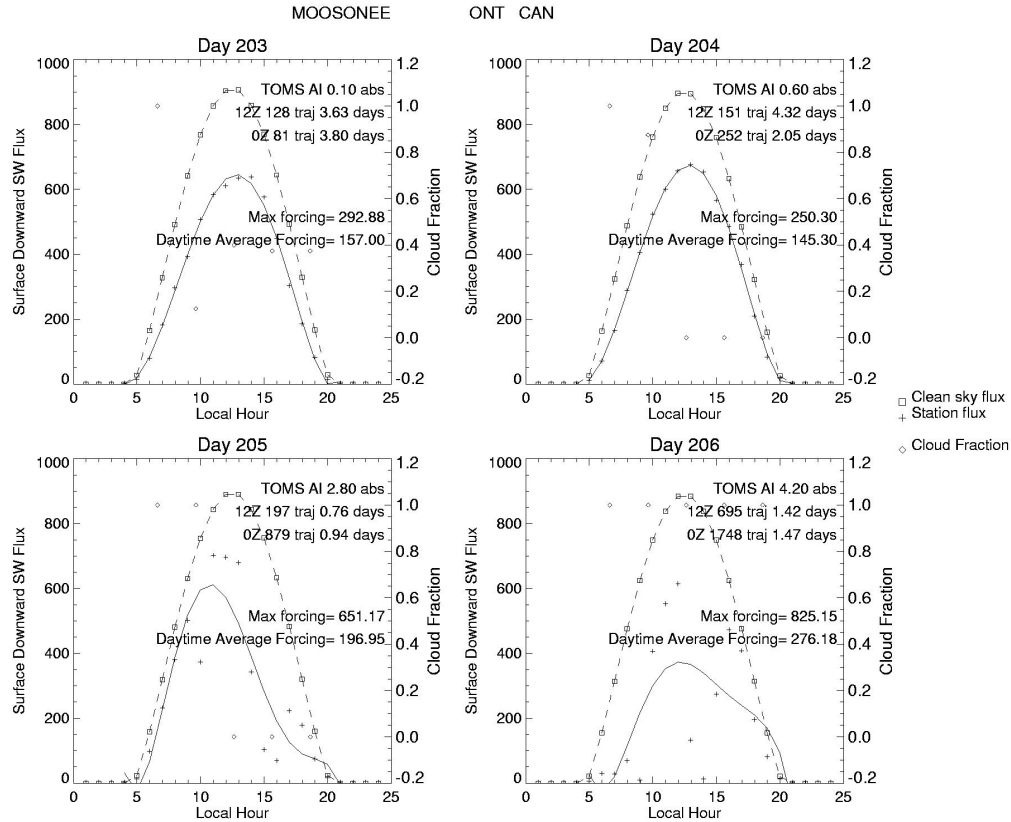


Fig. 2. As Figure 1, for Moosonee, ON. The station was covered by a mix of smoke and clouds during the latter two days of the period. Strong smoke forcing is seen for the first two days. Both trajectory analysis and the TOMS Aerosol Index show smoke over the station.

Site	Clean sky minus measured surface downward flux at solar noon (W/m2)	TOMS aerosol index	# trajectories from fire pixels
Winnipeg, MB	125	2.3/absorbing	423
Moosonee, ON	250	0.6/absorbing	403
Edmonton, AB	40	2.6/absorbing	0
Big Trout Lake, ON	228	4.7/absorbing	4731
Fredericton, NB	154	0.5/absorbing	138
Outlook, SK	20	5.2/absorbing	0

Table 2. Comparison of estimated surface shortwave smoke forcing with trajectory modeling and TOMS Aerosol Index. Outlook and Edmonton are west of the fire zone, and not considered to be smoke-covered. However, TOMS AI does see a strong aerosol signature at those sites for as yet unknown reasons. Big Trout Lake, Winnipeg, and Moosonee are within the fire region, where all methods agree that there is a strong smoke signature. Fredericton is far to the east of the fire zone, however trajectory modeling indicates a plume of smoke extending that far. This is seen by both TOMS and the surface radiometer data.

